



ELTE

FACULTY OF
INFORMATICS

BIOLOGICALLY INSPIRED ROBOTICS

Beáta Korcsok



ELTE | IK
DEPARTMENT OF
ARTIFICIAL
INTELLIGENCE



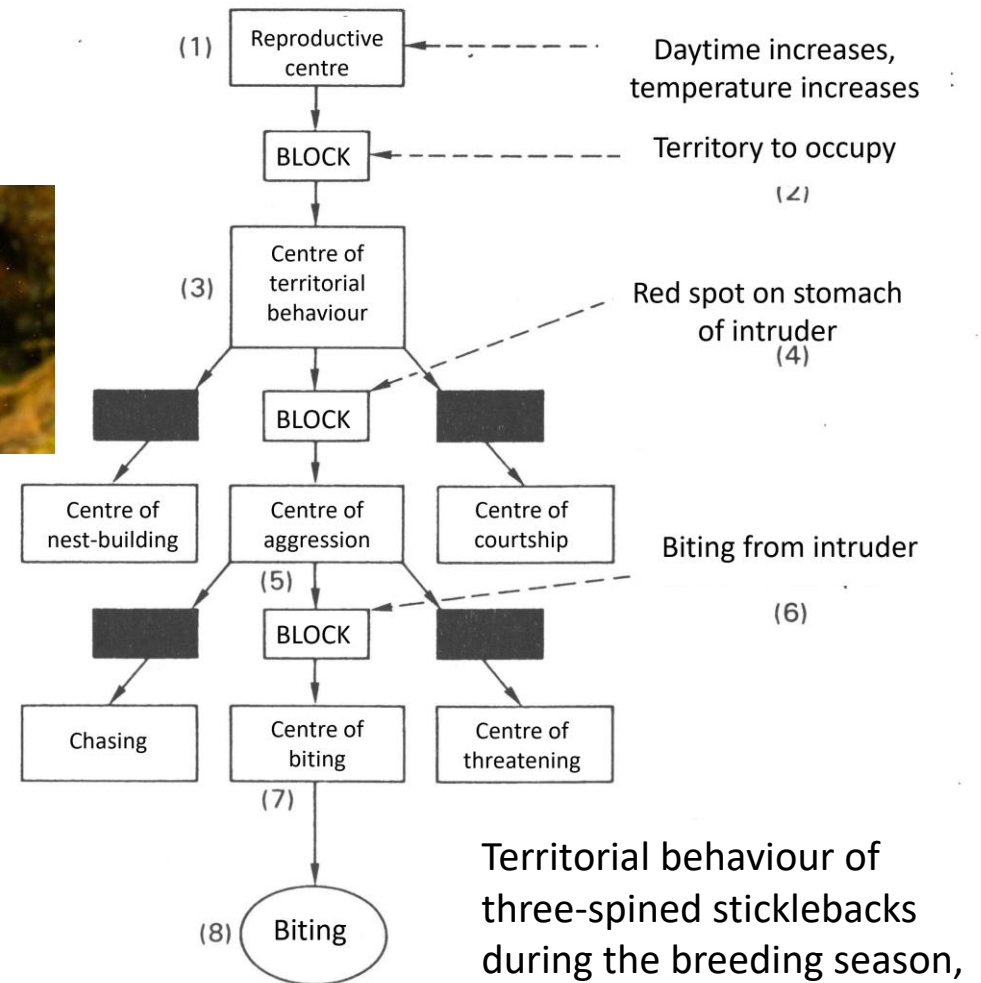
BOSCH

HUN-REN
Hungarian Research Network

Some slides contain explanations/article excerpts in the Notes section

JDE (*Jerarquía Dinámica de Esquemas*)

- JDE (Cañas & Matellán, 2007)
- Ethological approach
- Based on Tinbergen's hierarchical behavioural model
- Hierarchical
- Neural centres
- More and more specific centres, barriers (blocks) and key stimuli
- Action-specific „energy“ can accumulate in all centres (external stimuli, internal state, „energy“ flowing from higher centres)



Territorial behaviour of three-spined sticklebacks during the breeding season, based on Tinbergen's model (Csányi, 2002)

Territorial behaviour of three-spined sticklebacks



JDE

- JDE: Dynamic schema hierarchies
- Schema: a purposeful, independent execution process
- Off and on state, multiple input parameters, tunable, iterative, their state depends on higher-level schemas
- Perceptual and motor schemas
- Perceptual: 2 states, active or slept
- Motor: 4 states, slept, checking, ready or active

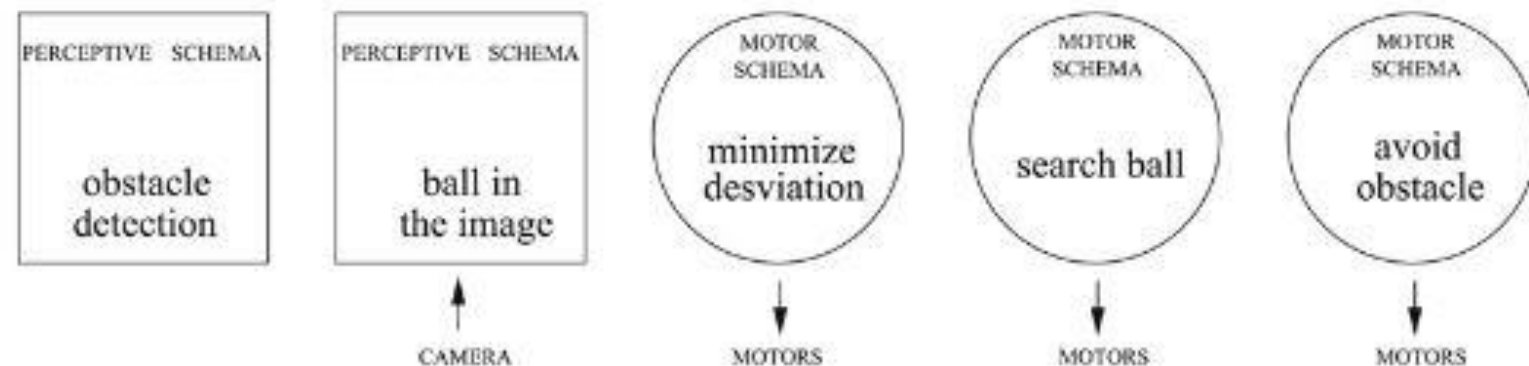


Fig. 5. Ball following completed by the avoiding obstacles' ability.

JDE

- The schema is in checking state, it monitors whether the necessary prerequisites for activation are met
- If yes, it goes into ready state → action selection competition (ASM) between ready schemas → the one that wins becomes active
- Activation from slept state to checking is only an option: a higher schema can activate several "sons" at the same time
- Entering into a real active state is determined by the competition between the environment and the schemas

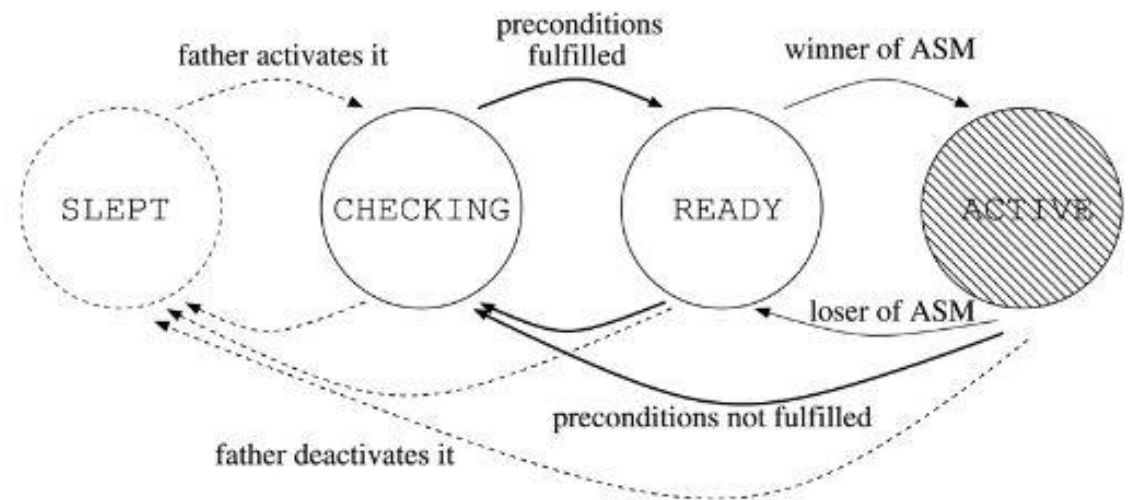


Fig. 6. Allowed transitions in the state of a motor schema.

JDE

- For the transition between checking and ready states, prerequisites must be fulfilled → schema activation region
- A higher schema modifies the activation region
- Preconditions: fulfilment of not a single condition, but a thresholded continuous variable which accumulates the contribution of different stimuli to the trigger
- Action Selection Mechanism (ASM)
- At each level of the hierarchy, there is a winner-takes-all competition between the motor schemas of the level
- New action selection at each iteration → quick response to environmental changes
- A new schema system is activated under a new winner

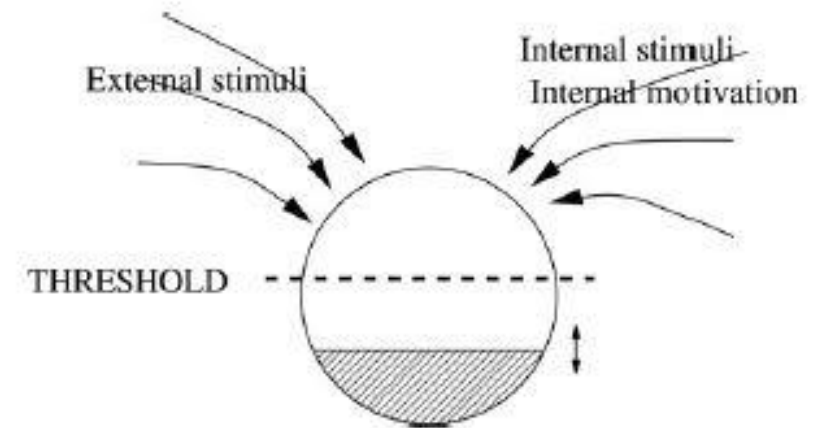


Fig. 9. Additive combination of stimuli in JDE.

JDE

- Only active schemas can send activation signals and modulating parameters to lower-level schemas
- Co-activation of schemas and continuous modulation
- Co-activation can be repeated recursively
- The chain of co-activation creates a specific hierarchy of schemas, resulting in global behaviour
- Hierarchies can be dynamically modified and rebuilt, depending on how the goals and conditions change under which a higher-level schema maintains the activation of a lower one
- → restricted variability: several alternatives are prepared at the same time, the most suitable of these will be selected



JDE

- Only the relevant perceptual schemas are active: selective attention to the environment → capacity optimization
- Motor schemas and the perceptual schemas they need are connected, but they can provide information to several motor schemas

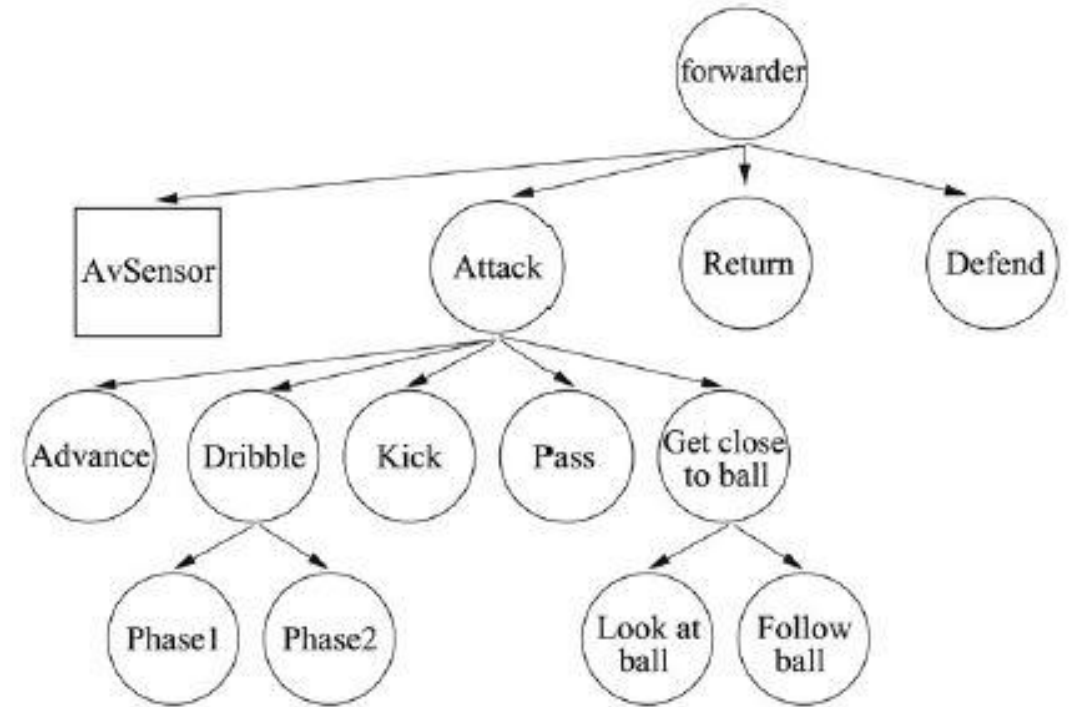


Fig. 14. Hierarchy of schemas to implement a robotic soccer player (only the forwarder role is shown).

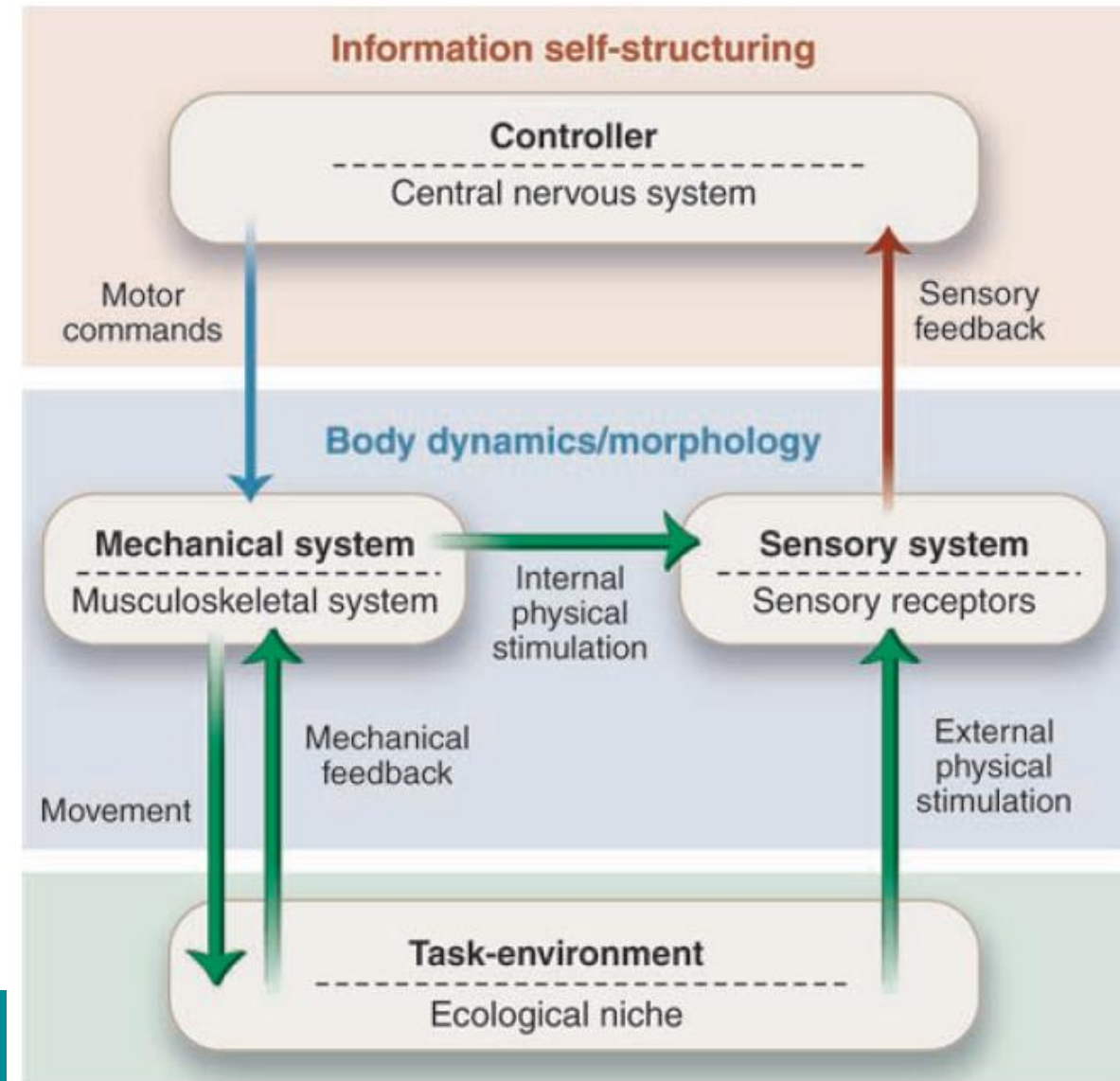
Self-organisation and embodiment

- Pfeifer et al., 2007
- Reciprocal and dynamical coupling between brain (control), body and environment
- A system's behaviour is affected by:
 - Its internal control structure (e.g., central nervous system)
 - The ecological niche in which the system is physically embedded
 - Its morphology (shape of its body and limbs, the type and placement of sensors and effectors)
 - The material properties of the elements composing the morphology
 - Physical constraints that shape the dynamics of the interaction of the embodied system with its environment



Self-organisation and embodiment

- Direct link between embodiment and information: coupled sensory-motor activity and body morphology induce statistical regularities in sensory input and within the control architecture → enhance internal information processing
- Embodied agent as a complex dynamical system → self-organization and emergence instead of hierarchical top-down control



Self-organisation and embodiment

- Classical robotics: centralized solutions where a microprocessor controls the movements of all limbs and joints
- Embodied perspective: distributes control and processing to all aspects of the agent (its central nervous system, the material properties of its musculoskeletal system, the sensor morphology, the interaction with the environment) e.g., grasping with fingertips
- ! • Embedded Neural Models
 - Physical interaction with the environment, realistic sensory inputs
 - Study models of natural neural information processing
 - Locomotion, navigation, orientation
 - Sensory-motor coordination: generation of information structure in sensory stimulation → spatiotemporal correlations in sensory input streams; redundancies between different perceptual modalities; regularities in sensory patterns that are invariant to illumination, size, orientation

Self-organisation and embodiment

- Learning:
- Cross-modal associations (e.g., seeing glass, predicting haptic input)
- Concept learning: e.g., glass: visual, haptic, proprioceptive sensory information



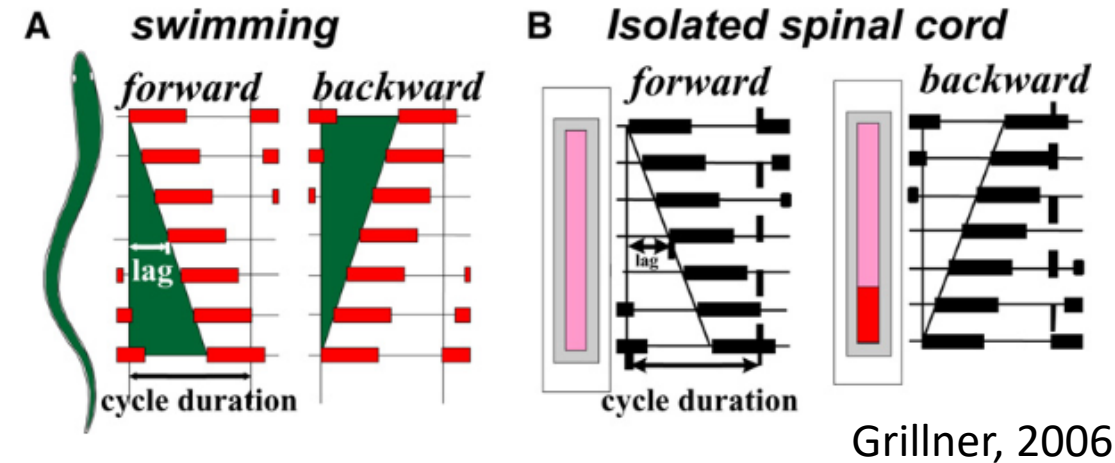
- Implications of embodiment
- Morphology, materials, sensory-motor interaction, self-stabilisation (e.g., insect walking: global communication between the legs, rapid adaptation to unpredictable bumps: passive compliance → e.g., pneumatic linear actuators, spring-damper systems)

60 cm/s, bouncing gate

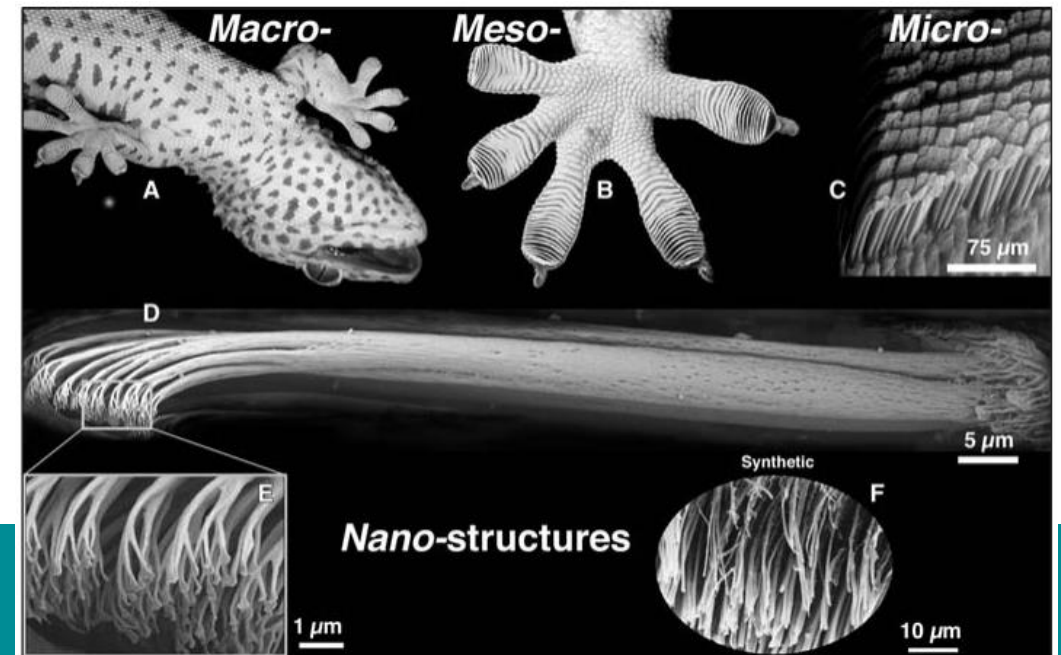


Self-organisation and embodiment

- Aquatic undulating locomotion in e.g. fish: traveling waves of neural activation transmitted along chains of coupled oscillators located in the spinal cord → torques propagating through individual segments

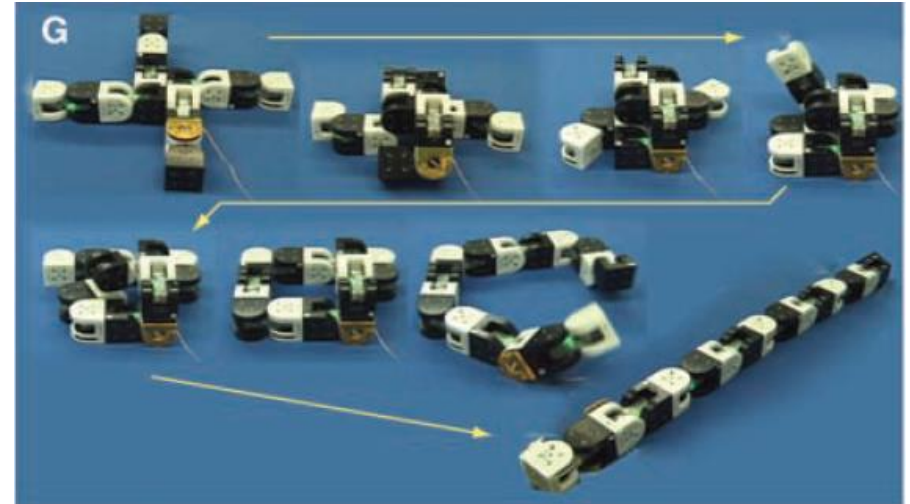


- Material characteristics
- E.g., fins, wings: resilience, stiffness, deformability
- Climbing: gecko feet → micropatterned fibrillar dry adhesives (van der Waals or capillary forces, Kwak & Kim, 2010)



Self-organisation and embodiment

- Morphology design
- Evolutionary robotics
- Generally: fixed morphology, evolve the robot controller (e.g. via neural networks)
- Biological systems: brain (controller) and body (morphology) coevolve
- Morphofunctional machines: devices that can change their functionality by a change in control AND by modifying their morphology
- Macroscopic modules composed of microprocessors, communication links, sensors, actuators, mechanical or magnetic docking interfaces
- Collective robotics: cooperating groups of robots



Multi-environment adaptive morphogenesis

- Baines et al., 2022
- Traditional rigid components & soft materials → augment the shape of limbs and shift robot gaits for multi-environment locomotion
- Animals that primarily inhabit one ecological niche tend to have specialized body plans & gait kinematics: increase locomotive efficiency in that niche, but degraded performance in other environments
- Semi-aquatic & semi-terrestrial animals display inherent morphological and gait compromises
- Amphibious robots:
e.g.,
bio-monitoring,
disaster response



Multi-environment adaptive morphogenesis

- Merge of specialized morphogenic features for aquatic and terrestrial locomotion: streamlined flipper shape and gaits (sea turtles) & columnar leg shape and gaits (terrestrial tortoises)
- Limbs capable of morphing between functional hydrodynamic and load-bearing shapes using variable-stiffness composites and various gaits
- Pneumatic actuators, thermoset polymer

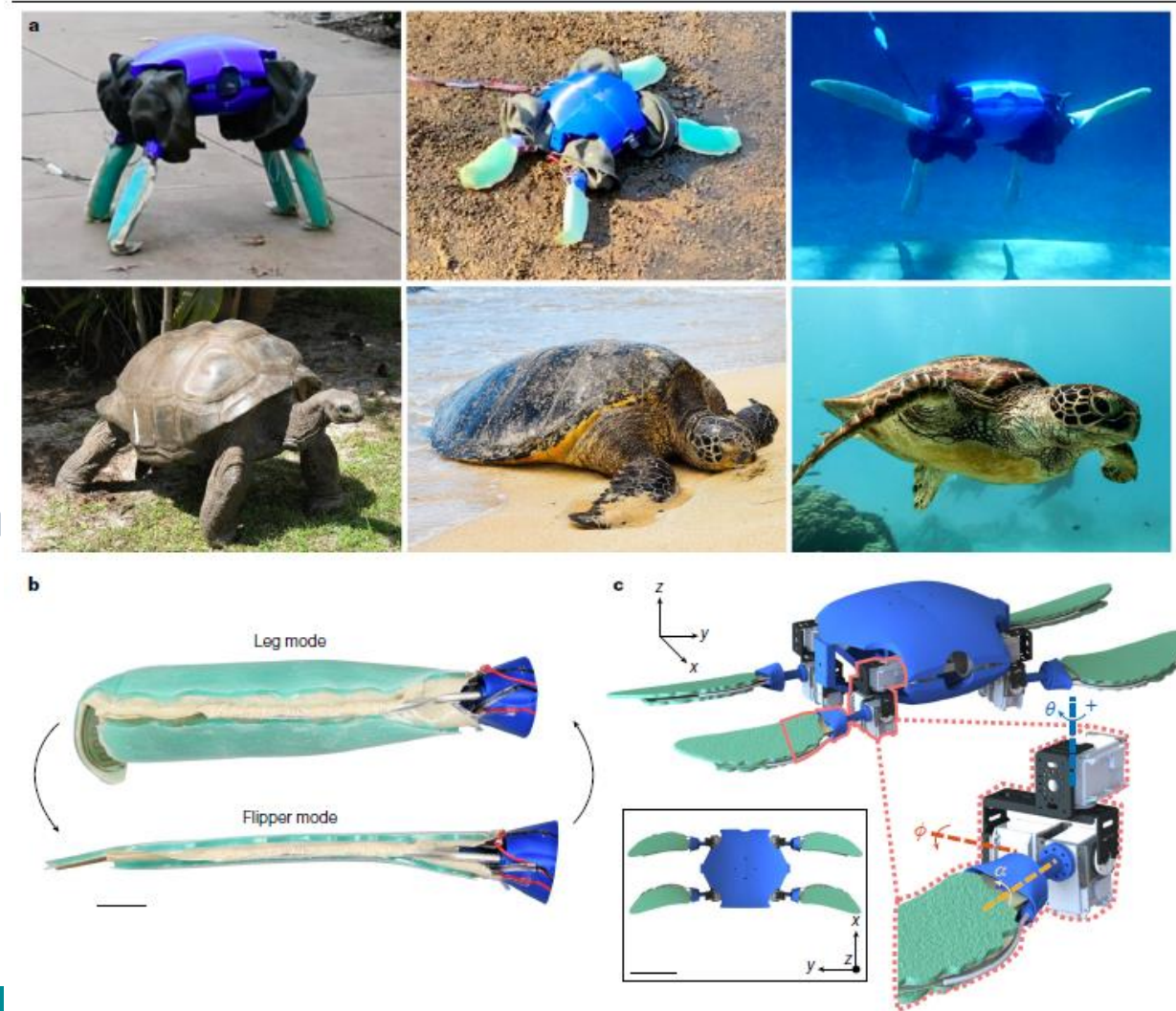
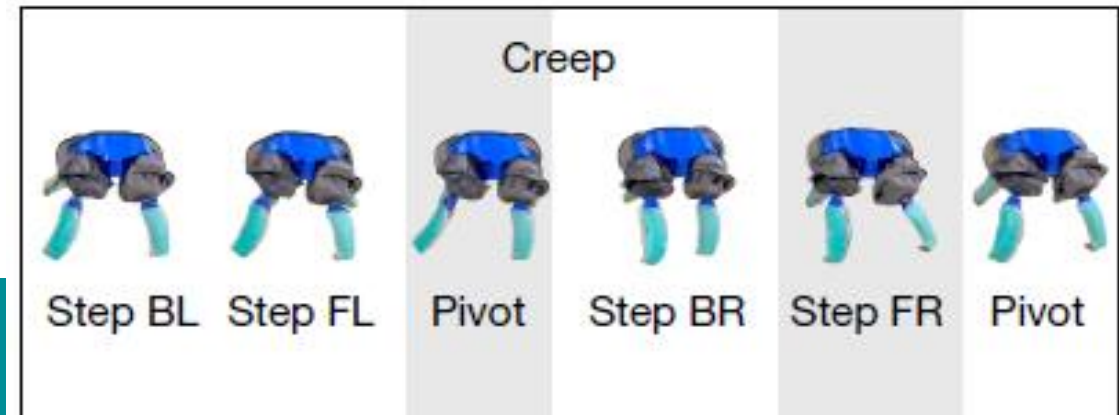
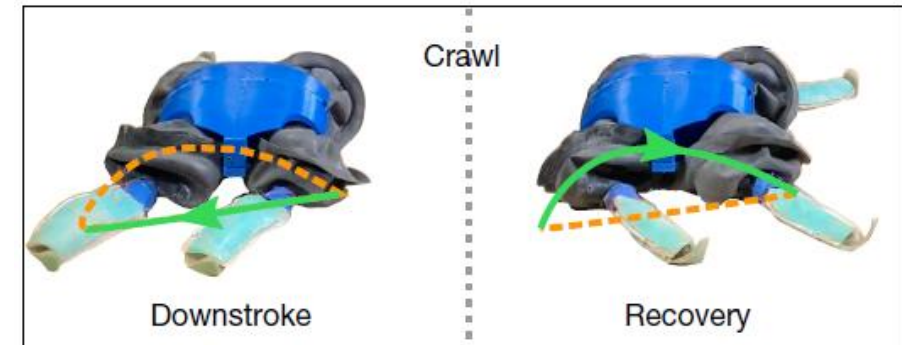
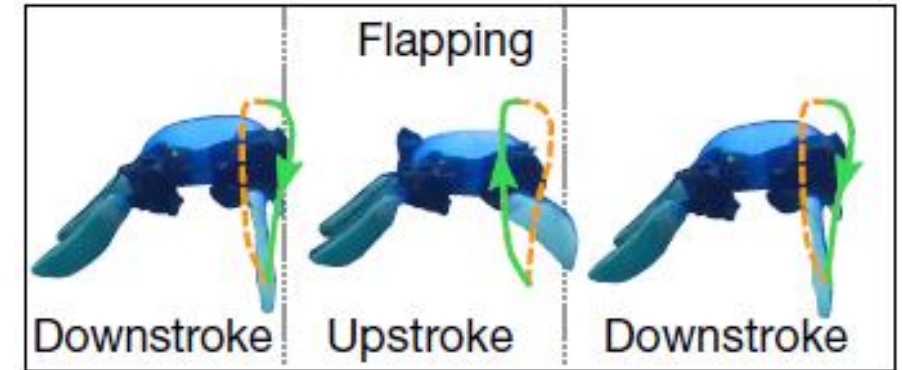
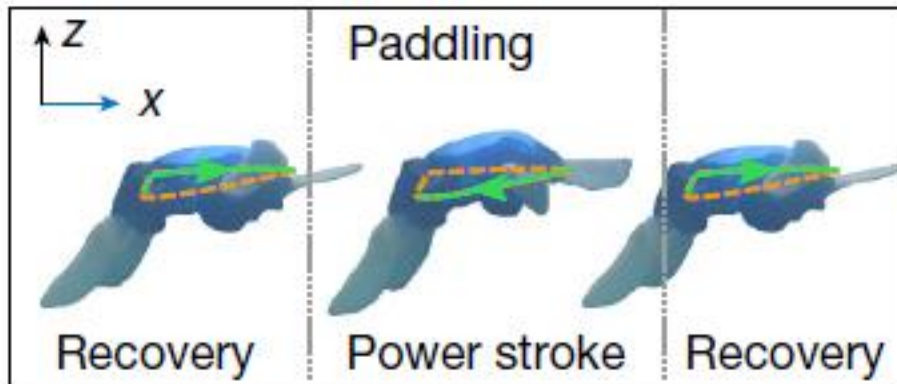


Fig. 1 | Turtle-inspired amphibious robot. **a**, ART replicates the limb shapes and gaits of highly adapted turtle species, and is a platform capable of specialized locomotion modes for transition between aquatic and terrestrial habitats. **b**, Side view of the morphing limb. Scale bar, 30 mm. **c**, Isometric and

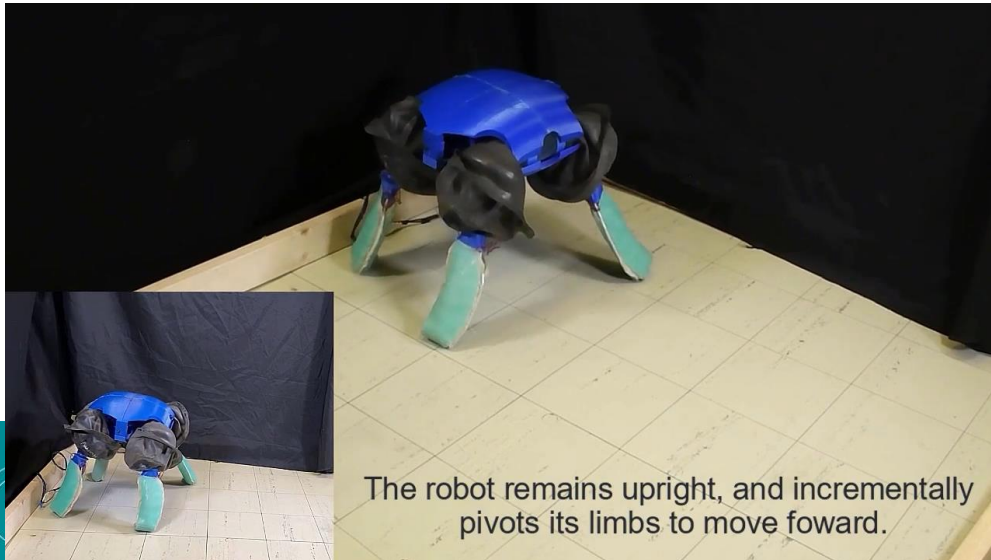
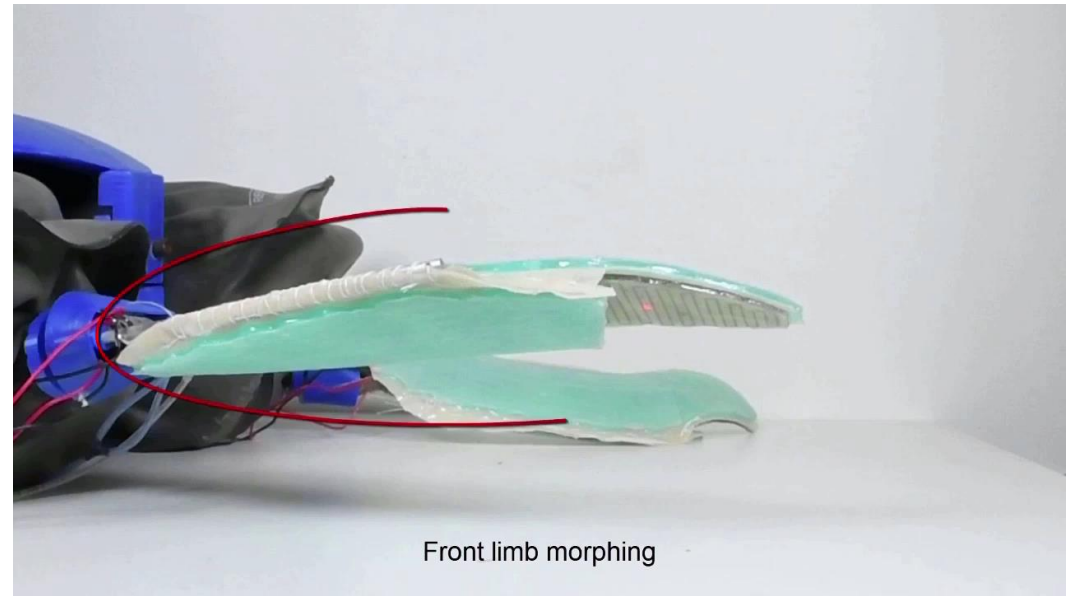
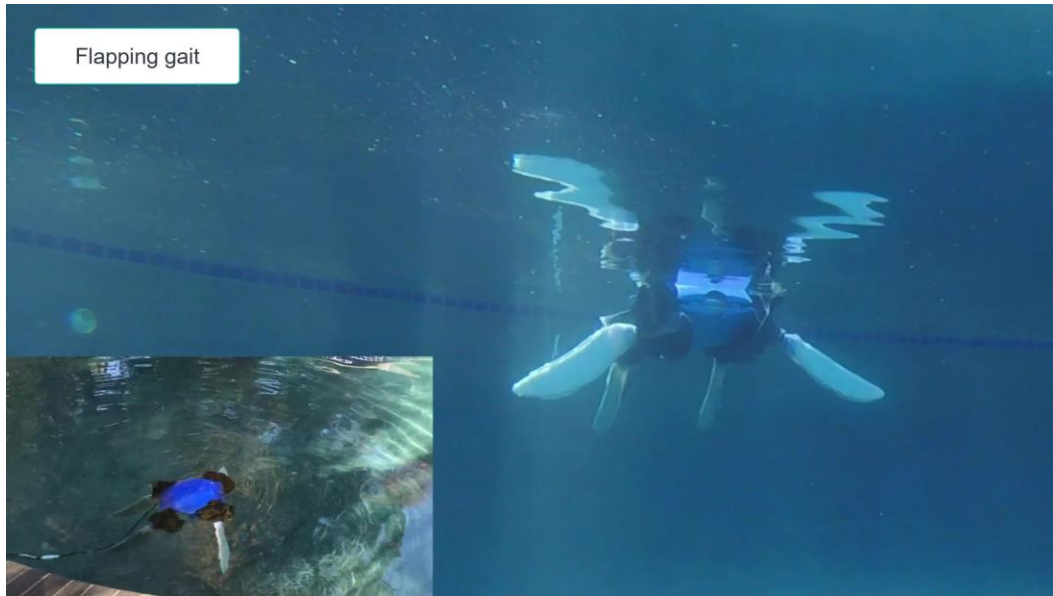
top views of the robot computer-aided-design model. Scale bar, 0.16 m. The inset shows the joint arrangement. The joints are typically clad in rubber bellows, removed here for visualization. θ , ϕ and α are axes for forwards and backwards, up and down, and angle-of-attack movements, respectively.

Multi-environment adaptive morphogenesis

- Chassis (electronics), shell (streamlining, buoyancy tuning, payload storage, protection), shoulder joints, morphing limbs
- Buoyancy adjusted for surface and submerged swimming



Multi-environment adaptive morphogenesis

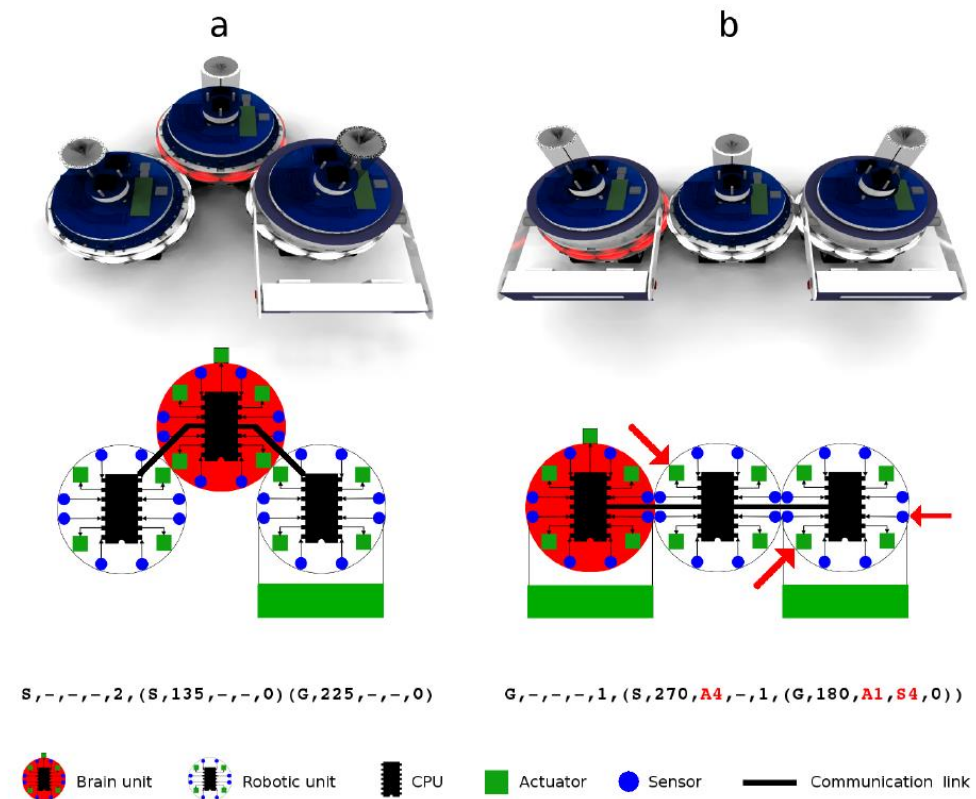


Modular robots with mergeable nervous systems

- Mathews et al., 2017
- Modular approach: robots with different capabilities, shapes, sizes could construct and reconfigure themselves
- Current modular robots: robotic units remain individually autonomous and rely on distributed approaches for coordination
- No nervous system that spans the whole body and transforms a composite system into a single entity → limited sensorimotor coordination
- Mergeable Nervous System (MNS) robots
- Connected robotic units; robot responsible for centralised decision making → brain unit
- Self-assembling multirobot system displays sensorimotor coordination equivalent to that observed in monolithic robots

Modular robots with mergeable nervous systems

- Physical connection topology: rooted tree
- Logical topology follows the physical connection topology with each constituent robotic unit: recursive body representation of itself and all of its child robotic units (storing relative positions and hardware configurations)
- When a merge between two robots occurs, only a single message needs to be passed up the nervous system to the brain unit
- Information in the message is incrementally updated by each intermediate unit with local topological information (sensing, actuation and computational capabilities)



Supplementary Fig. 2: Brain units' internal representation of robot morphology. (a,b)

Modular robots with mergeable nervous systems

- Control logic
- Expressed in high-level logic that is independent of the size and shape of the robot
- If a high-level command applies to a robotic unit, the robot nervous system locally translates the command into instructions for the unit's actuators
- Spatial references are translated into the frame of reference of the receiving unit before the messages are transmitted (wi-fi; infrared & radio)

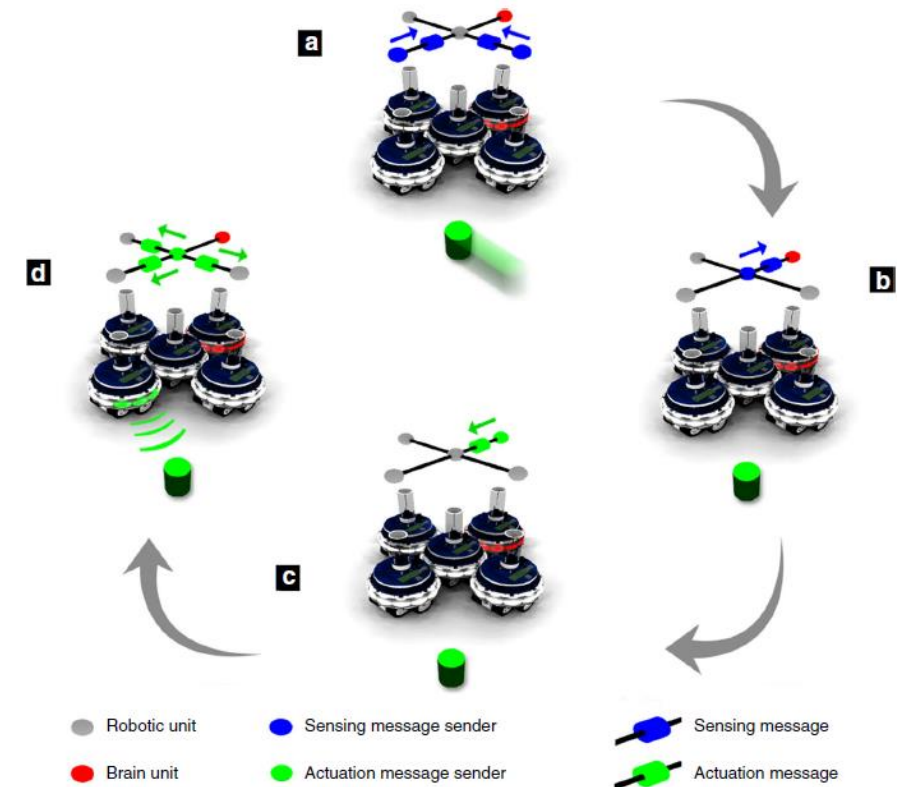


Fig. 4 Sensor and actuator information flow in an MNS robot. A 5-unit MNS robot detects and then responds to a stimulus. a: The stimulus moves within sensor range of two robotic units in the MNS robot. Both robotic units perform the computationally intensive visual image processing required to analyze their camera feeds. They pass an abstraction of this information (e.g., existence and coordinates of the stimulus) up to their parent robotic unit (i.e., the unit in the center of the robot) using a Wi-Fi connection. b: The parent robotic unit fuses the information coming from two of its child robotic units, to form a more accurate estimate of the stimulus' coordinates. The parent robotic unit then passes this single item of information up to its own parent robotic unit, which in this case is the brain unit. The brain unit decides what action to take, based on the data it has received—in this case, the decision is to point at and retreat from the stimulus. c: The brain unit issues high-level actuator commands. d: The high-level commands are translated into actuator instructions individually by each robotic unit

Modular robots with mergeable nervous systems

- Indicating stimulus location, avoidance from close stimulus

Mergeable Nervous Systems for Robots

Nithin Mathews,¹ Anders Lyhne Christensen,² Rehan O'Grady,¹ Francesco Mondada,³ Marco Dorigo¹

Video 2: Morphology and size independent reactions to an external stimulus

¹IRIDIA, Université Libre de Bruxelles, Brussels, Belgium

²BioMachines Lab, Instituto Universitário de Lisboa (ISCTE-IUL), Lisbon, Portugal

³EPFL-LSRO, Ecole polytechnique fédérale de Lausanne, Lausanne, Switzerland

Modular robots with mergeable nervous systems

- Heartbeat protocol for fault detection

Mergeable Nervous Systems for Robots

Nithin Mathews,¹ Anders Lyhne Christensen,² Rehan O'Grady,¹ Francesco Mondada,³ Marco Dorigo¹



Video 3: Borrowing object lifting capabilities

¹IRIDIA, Université Libre de Bruxelles, Brussels, Belgium

²BioMachines Lab, Instituto Universitário de Lisboa (ISCTE-IUL), Lisbon, Portugal

³EPFL-LSRO, Ecole polytechnique fédérale de Lausanne, Lausanne, Switzerland



Mergeable Nervous Systems for Robots

Nithin Mathews,¹ Anders Lyhne Christensen,² Rehan O'Grady,¹ Francesco Mondada,³ Marco Dorigo¹



Video 4: Self-healing

¹IRIDIA, Université Libre de Bruxelles, Brussels, Belgium

²BioMachines Lab, Instituto Universitário de Lisboa (ISCTE-IUL), Lisbon, Portugal

³EPFL-LSRO, Ecole polytechnique fédérale de Lausanne, Lausanne, Switzerland

Continuous Self-Modeling

- Bongard et al., 2006
- Ability to operate after injury by creating qualitatively different compensatory behaviours
- How a robot can learn its own morphology if it cannot be inferred by direct observation or retrieved from a database of past experiences
- Physical trial and error, but requires hundreds of tests on the physical machine → generally too slow, energetically costly, risky
- Active process of autonomous & continuous self-modelling
- Indirectly infer its own morphology through self-directed exploration → use the resulting self-models to synthesize new behaviours
- Continuously diagnose and recover from damage
- Three algorithmic components that are executed continuously by the physical robot: modelling, testing, and prediction

Continuous Self-Modeling

- 1. Robot performs random motor action, records resulting sensory data
- 2. The model synthesis component synthesizes 15 candidate self-models using stochastic optimization to explain the observed sensory-actuation causal relationship
- 3. The action synthesis component uses these models to find a new action most likely to elicit the most information from the robot
- 4. Robot performs new action, reiteration *16
- 5. The most accurate model is used by the behaviour synthesis component to create a desired behaviour

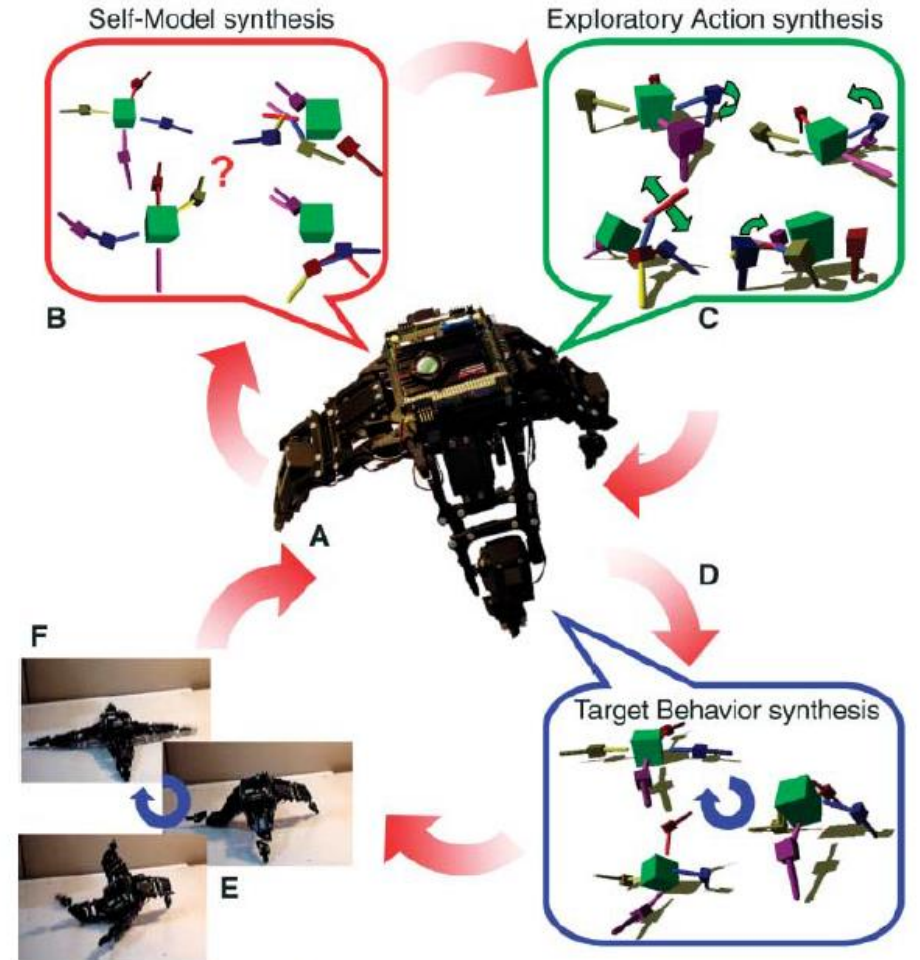


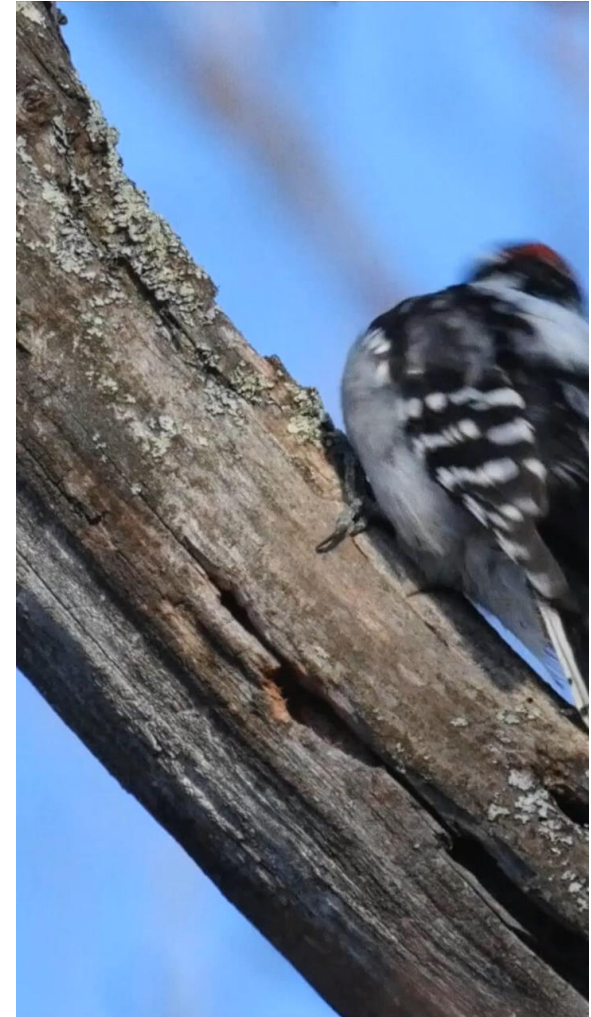
Fig. 1. Outline of the algorithm. The robot continuously cycles through action execution. (A and B) Self-model synthesis. The robot physically performs an action (A). Initially, this action is random; later, it is the best action found in (C). The robot then generates several self-models to match sensor data collected while performing previous actions (B). It does not know which model is correct. (C) Exploratory action synthesis. The robot generates several possible actions that disambiguate competing self-models. (D) Target behavior synthesis. After several cycles of (A) to (C), the currently best model is used to generate locomotion sequences through optimization. (E) The best locomotion sequence is executed by the physical device. (F) The cycle continues at step (B) to further refine models or at step (D) to create new behaviors.

Continuous Self-Modeling

Stage I:
Generating internal models

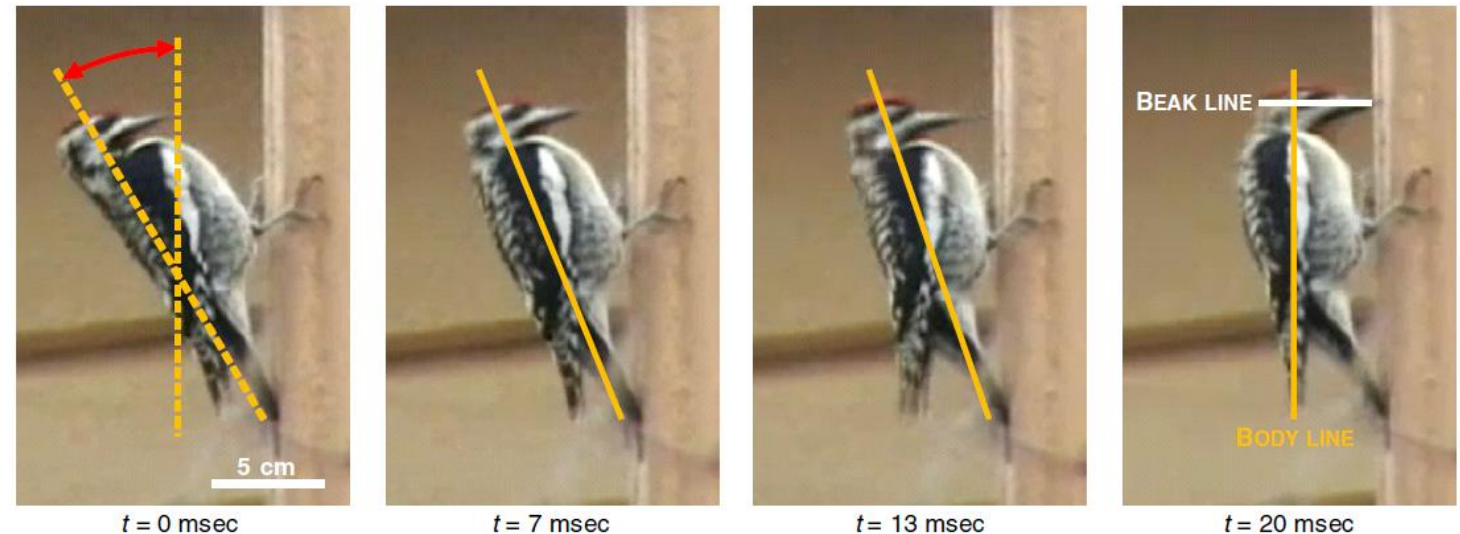
Woodpecker head anatomy → shock-absorbing system

- Yoon & Park, 2011
- Golden-fronted woodpecker (*Melanerpes aurifrons*)
- Drumming on wood: 18-22 times/sec
- 1200 g deceleration, 500-600 repetitions/day
- No major brain damage or loss of consciousness
- Challenge of mechanical shock above 10kHz and 1000 g in micromachined devices
- Early solutions:
 - 1. Shock attenuators (SA): damp all mechanical excitations over all frequencies
 - Viscoelastic SA: degrades at low and high temperature



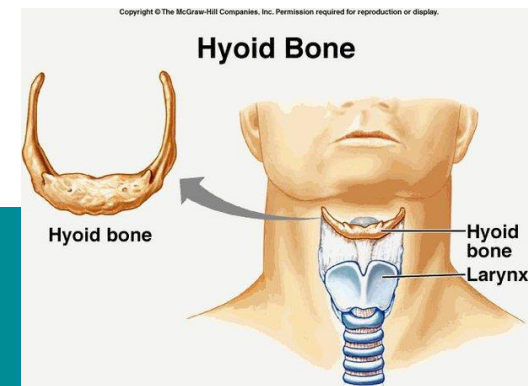
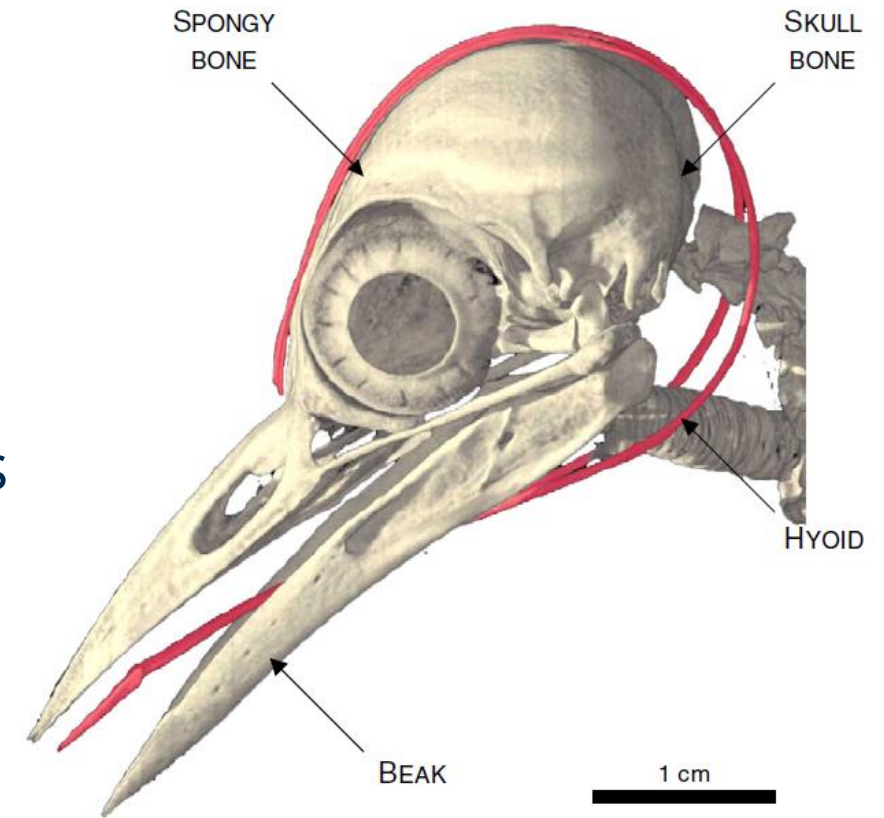
Woodpecker head anatomy → shock-absorbing system

- Fluid SA: too big
- Non-obstructive particle damping SA: needs bigger objects
- 2. Shock low-pass filters: pass low-frequency mechanical excitations but attenuate high-frequency ones: not frequently used
- Biomimetic approach
- Anatomy, physiology
- Drumming posture: beak line and body line are perpendicular, no head rotation → reducing shear force



Woodpecker head anatomy → shock-absorbing system

- Head anatomy
- Based on X-ray computed tomography (CT) images
- Large beak
- Hyoid: attachment site for throat and tongue muscles, helps extending the tongue, distributes mechanical excitations, reinforces head
- Spongy bone: dense but spongy, distributes mechanical excitations
- Tightly packed skull, narrow space for cerebrospinal fluid (CSF) → reducing the transmission of the mechanical excitations into the brain through the CSF

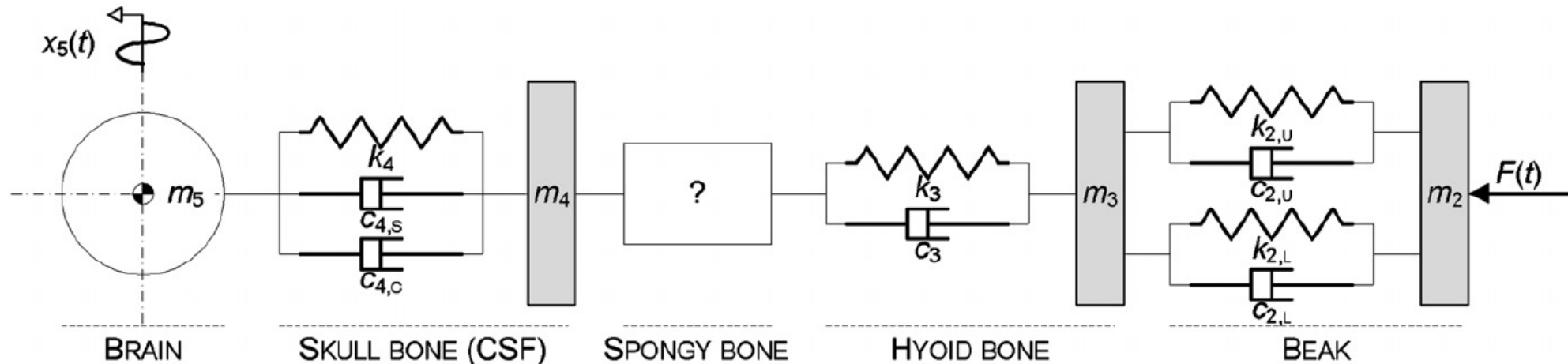


Woodpecker head anatomy → shock-absorbing system



Woodpecker head anatomy → shock-absorbing system

- Kinematic model of the bird's drumming motion & mechanical vibration analysis
- Mass-damper-spring model (m : mass, c : damping coefficient, k : stiffness x : displacement under external force $F_{(t)}$)
- Spongy bone: empirical analysis



Woodpecker head anatomy → shock-absorbing system

Table 2. Parameters used in the mechanical vibration analysis.

Structure	Parameter	Symbol	Value	Reference
Woodpecker	Drumming distance	S_0	7×10^{-2} m	Vincent <i>et al</i> 2007
	Drumming frequency	f_d	25 Hz	Stark <i>et al</i> 1998, Vincent <i>et al</i> 2007
	Striking velocity	v_s	3.6 m s^{-1}	Vincent <i>et al</i> 2007
	Penetrating time ^a	t_p	2×10^{-3} sec	–
	Head mass	m_h	9×10^{-3} kg	Vincent <i>et al</i> 2007
Tree	Stiffness	k_1	1000 N m^{-1}	Moore and Maguire 2004
	Damping coefficient	c_1	10 N·s m^{-1}	Moore and Maguire 2004
Beak	Length	l_2	2.6×10^{-2} m	DigiMorph Staff 2004
	Diameter	d_2	6×10^{-3} m	DigiMorph Staff 2004
	Density ^b	ρ_2	1456 kg m^{-3}	Oda <i>et al</i> 2006
	Young's modulus ^c	E_2	3×10^7 Pa	Seki <i>et al</i> 1998
	Damping coefficient ^d	$\text{Tan } \delta$	0.032	Fortis <i>et al</i> 2004
Hyoid	Length	l_3	6.67×10^{-2} m	DigiMorph Staff 2004
	Height	h_3	6.5×10^{-4} m	DigiMorph Staff 2004
	Width	w_3	6.5×10^{-4} m	DigiMorph Staff 2004
	Density ^e	ρ_3	1200 kg m^{-3}	Oda <i>et al</i> 2006
	Young's modulus ^f	E_3	1.5×10^9 Pa	Alexander <i>et al</i> 1977
	Damping coefficient ^e	ζ	0.25	Revel <i>et al</i> 2003
Skull bone with cerebrospinal fluid (CSF)	Diameter	d_4	2×10^{-2} m	DigiMorph Staff 2004
	Thickness	t_4	2.5×10^{-3} m	DigiMorph Staff 2004
	Density	ρ_4	1456 kg m^{-3}	Oda <i>et al</i> 2006
	Young's modulus	E_4	8.75×10^9 Pa	Oda <i>et al</i> 2006
	Poisson's ratio	ν	0.2	Oda <i>et al</i> 2006
	CSF viscosity ^g	μ	$8.5 \times 10^{-4} \text{ N·s m}^{-1}$	Oda <i>et al</i> 2006
Brain	Diameter	d_5	1.5×10^{-2} m	DigiMorph Staff 2004
	Density	ρ_5	1040 kg m^{-3}	Oda <i>et al</i> 2006

^a Calculated from the drumming frequency.

^b Data from woodpecker cranium.

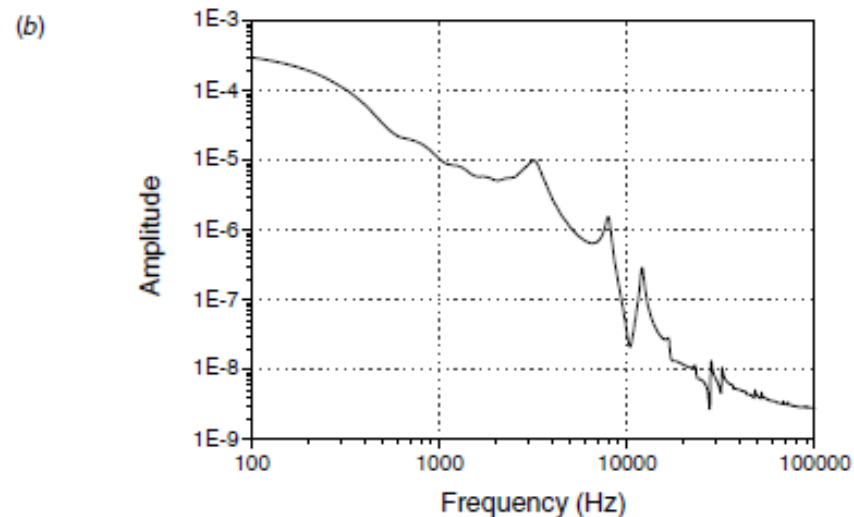
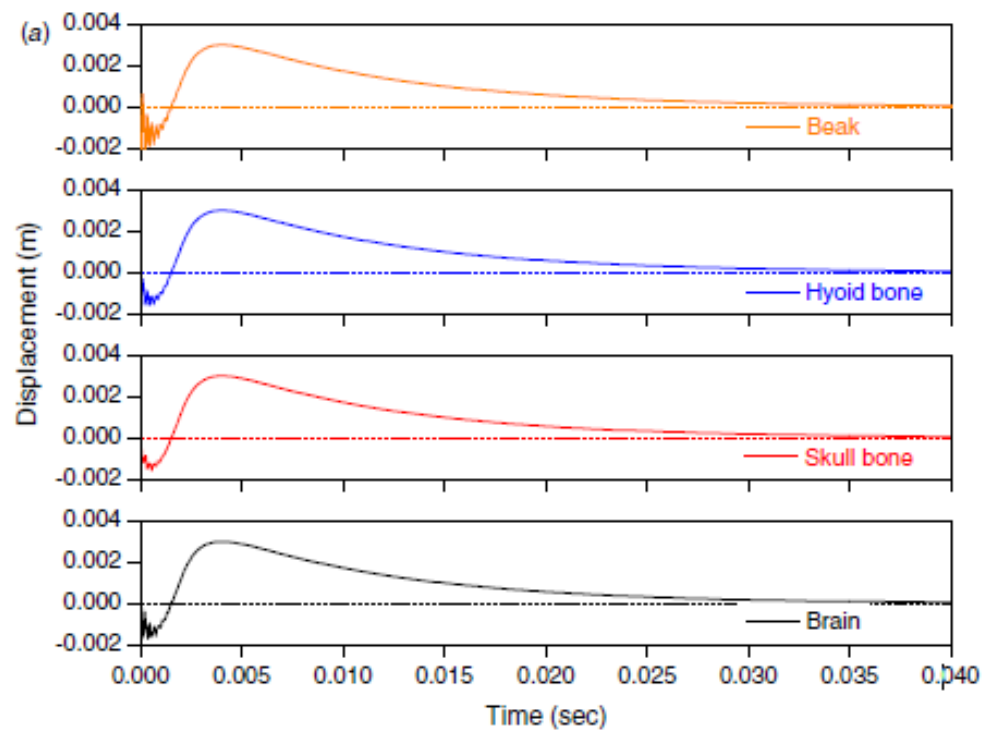
^c Data from toucan beak.

^d Data from human skull bone.

^e Data from human tendon.

^f Data from mammal tendon.

^g Data from human CSF.



- Assumption: spongy bone acts as a mechanical low-pass filter, eliminating the initial high-frequency vibrations

Figure 6. Mechanical vibration analysis of a woodpecker (beak, hyoid, skull bone, and brain) under drumming impact without considering the spongy bone. (a) Dynamic response. (b) Frequency spectrum diagram of the dynamic response of a brain. The relatively high-frequency vibrations of the brain during $t = 0$ to 2 ms, which can cause g-force-induced loss of consciousness or brain damage to the woodpecker, indicate that the spongy bone eliminates the initial high-frequency vibrations as a mechanical low-pass filter.

Woodpecker head anatomy → shock-absorbing system

- Modeling the spongy bone
- Close-packed SiO_2 microglasses (→ modeling porous material)
- In aluminium enclosure with accelerometer
- Vertically and randomly vibrated by the vibration exciter (10 g and up to 25 kHz)
- The measured vibration transmissibility shows the porous structure with resilience rigidity absorbs mechanical excitations with higher frequency than a cut-off frequency which is determined by the diameter of the microglasses.

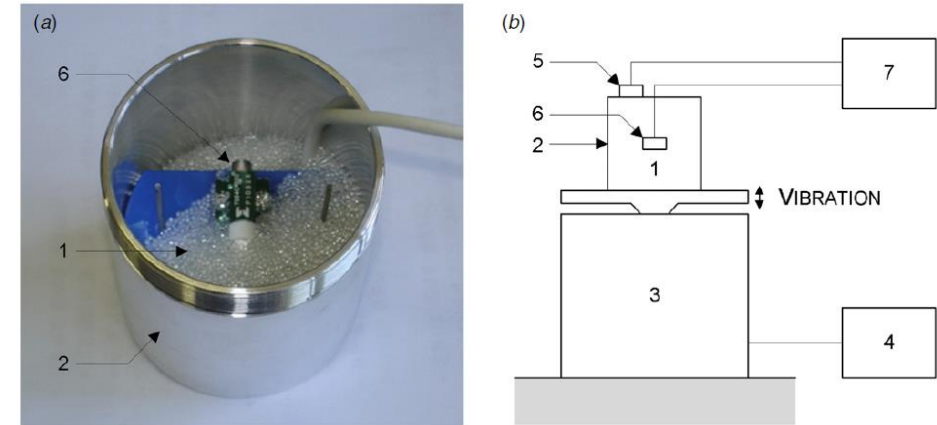
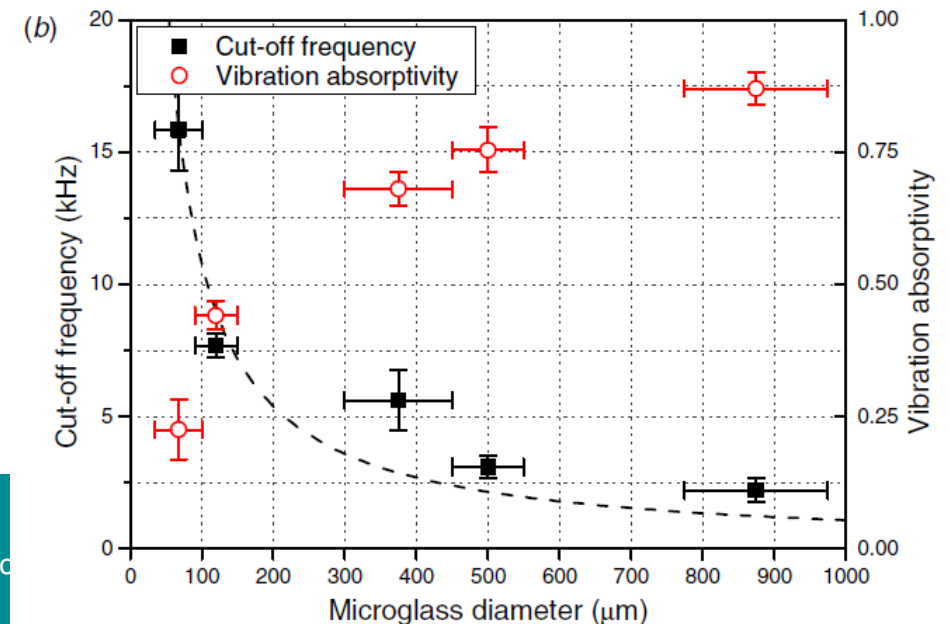


Figure 7. Experimental setup for empirical characterization of the spongy bone. (a) Enlarged view of the aluminum enclosure, showing microglasses and a reference accelerometer. (b) Experimental apparatus consisting of (1) microglasses, (2) aluminum enclosure, (3) vibration exciter, (4) power amplifier and signal generator, (5) reference accelerometer, (6) measurement accelerometer, (7) data recorder.



Woodpecker head anatomy → shock-absorbing system

- Similarly to the microglasses, the spongy bone is believed to transmit 90–99% lower frequency & absorb 90–99% higher frequency than the spongy bone's cut-off frequency
- Bio-inspired shock-absorbing system
 1. an external layer with high strength, protecting the micromachined devices from physical damage → beak
 2. a viscoelastic layer which evenly distributes incident mechanical excitations → hyoid
 3. a porous structure with resilience rigidity, suppressing high-frequency mechanical excitations & preventing transmitted ones from being concentrated into the micromachined devices → spongy bone
 4. another high-strength layer with porous structure → skull

Woodpecker head anatomy → shock-absorbing system

- Optimal dimension parameters, particle-filling ratio and materials
- 60 mm air-gun experiment → g force tolerance
- Comparison with commercial hard resin SA system
- Micromachines: e.g., diodes, capacitors, optocouplers
- Mechanical excitations of 20 000 to 60 000 g

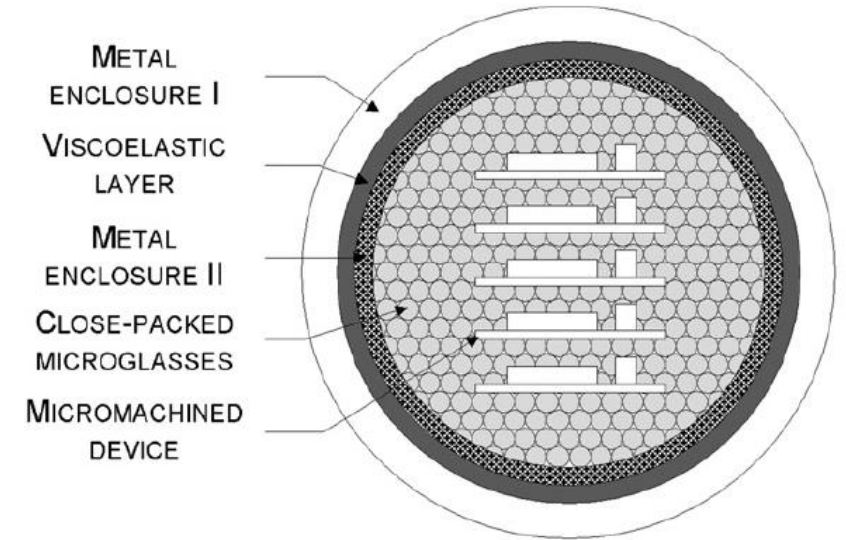


Table 4. 60 mm air-gun experiment results of the bio-inspired shock-absorbing system, compared to those of the hard resin shock-absorbing system.

Device	Package type	Failure rate (%)											
		Bio-inspired shock-absorbing system						Hard resin shock-absorbing system					
		20 000 g		40 000 g		60 000 g		20 000 g		40 000 g		60 000 g	
SCR	Lead	0	(0/36)	0	(0/36)	0	(0/36)	0	(0/36)	0	(0/36)	13.9	(5/36)
	SMD	0	(0/28)	0	(0/28)	0	(0/28)	0	(0/28)	0	(0/28)	0	(0/28)
Diode	Lead	0	(0/144)	0	(0/144)	0.7	(1/144)	0	(0/144)	5.6	(8/144)	26.4	(38/144)
	SMD	0	(0/104)	0	(0/104)	0	(0/104)	0	(0/104)	0	(0/104)	9.6	(10/104)
Optocoupler	DIP	0	(0/48)	0	(0/48)	0	(0/48)	0	(0/48)	6.3	(3/48)	22.9	(11/48)
Capacitor	SMD	0	(0/44)	0	(0/44)	0	(0/44)	0	(0/44)	0	(0/44)	6.8	(3/44)

Woodpecker (<i>Melanerpes aurifrons</i>)	Bio-inspired shock-absorbing system
Beak	Metal (steel) enclosure I
Hyoid	Viscoelastic layer (rubber)
Spongy bone	Close-packed microglass
Skull bone with CSF	Metal (aluminum) enclosure II
Brain	Micromachined devices

References

- Autumn, K. (2007). Gecko adhesion: structure, function, and applications. *MRS bulletin*, 32(6), 473-478.
- Baines, R., Patiballa, S. K., Booth, J., Ramirez, L., Sipple, T., Garcia, A., ... & Kramer-Bottiglio, R. (2022). Multi-environment robotic transitions through adaptive morphogenesis. *Nature*, 610(7931), 283-289.
- Bongard, J., Zykov, V., & Lipson, H. (2006). Resilient machines through continuous self-modeling. *Science*, 314(5802), 1118-1121.
- Cañas, J. M., & Matellán, V. (2007). From bio-inspired vs. psycho-inspired to etho-inspired robots. *Robotics and Autonomous Systems*, 55(12), 841-850.
- Csányi, V. (2002). Etológia. *Nemzedékek Tudása Tankönyvkiadó*
- Grillner, S. (2006). Biological pattern generation: the cellular and computational logic of networks in motion. *Neuron*, 52(5), 751-766.
- Mathews, N., Christensen, A. L., O'Grady, R., Mondada, F., & Dorigo, M. (2017). Mergeable nervous systems for robots. *Nature communications*, 8(1), 439.
- Pfeifer, R., Lungarella, M., & Iida, F. (2007). Self-organization, embodiment, and biologically inspired robotics. *science*, 318(5853), 1088-1093.
- Yoon, S. H., & Park, S. (2011). A mechanical analysis of woodpecker drumming and its application to shock-absorbing systems. *Bioinspiration & Biomimetics*, 6(1), 016003.



ELTE

FACULTY OF
INFORMATICS

Thank you for your attention!

Korcsok Beáta
korcsokbea@gmail.com

